

32. COMPARISONS BETWEEN THE OXYGEN ISOTOPIC COMPOSITION OF PORE WATER AND *GLOBIGERINOIDES RUBER* IN SEDIMENTS FROM HOLE 817C¹

Peter K. Swart²

ABSTRACT

The oxygen isotopic composition of pore waters squeezed from sediments in Hole 817C co-varies with the oxygen isotopic composition of *Globigerinoides ruber* below 8 mbsf. The magnitude of the variation in the pore water $\delta^{18}\text{O}$ is approximately 30% of the variation in the foraminifers. Overall, the $\delta^{18}\text{O}$ of the pore waters increases down the core, a trend that is also present in the Cl^- concentrations. The variations in the $\delta^{18}\text{O}$ of pore waters may be the result of either of two phenomena. First, these may reflect original variations in the waters, the magnitude of which has been subsequently reduced by process of diffusion. Second, these may reflect recrystallization of the precursor sediment and isotopic exchange between the fluids and the recrystallized sediment. At the moment data are not available to ascertain which process is responsible although the correlation between the Cl^- and the $\delta^{18}\text{O}$ data suggests that these values reflect the original composition modified by diffusion.

INTRODUCTION

The oxygen and hydrogen isotopic compositions of water contained in the interparticle pore space of buried sediment are initially similar to those of the bottom water at the time of deposition. With increasing age, the O and H isotopic compositions of the entrained water can be altered by (1) diagenetic interactions with the sediment, (2) mixing with waters deposited at different time periods, and/or (3) diffusion along concentration gradients. The importance of these effects has been studied by numerous researchers and was recently reviewed by Lawrence (1989). This study examines the $\delta^{18}\text{O}$ composition of pore water contained in sediments from Hole 817C and discusses the potential importance of each of these processes for altering the oxygen isotopic composition of the pore fluids.

SCIENTIFIC BACKGROUND

Hole 817C is situated on the northern side of the Townsville Trough in 1016.1 m of water (Fig. 1). Although no sedimentological descriptions were performed for this core, it can be considered to be identical to the upper portion of Holes 817A, 817B, and 817D. Drilling in Hole 817C penetrated 26.9 m of homogeneous micritic ooze, which was squeezed at 10-cm intervals, yielding a total of 269 samples that were processed for interstitial water analyses. The entire core is latest Pleistocene in age. The boundary between Zones CN15 and CN14b in Hole 817A was given as lying between the bottom of Cores 133-817A-1H and -2H, and the boundary between Zones CN14b and CN-14a between Cores 133-817A-3H and -4H. Later research by Gartner (this volume) refined these age boundaries to 0.275 Ma at 25.08 mbsf and 0.465 Ma at 28.07 mbsf. Further age control is presented here.

METHODS

Sediment samples were squeezed on board the *JOIDES Resolution* using the conventional methods (Manheim and Sayles, 1972). After filtration, samples were analyzed for alkalinity and chloride. A portion of the sample was subsequently sealed in a glass ampule for

later O isotopic analyses. The oxygen isotopic composition was determined on CO_2 equilibrated with 1 cm^3 of sample in a water bath at 25°C for 24 to 36 hr (after the method of Epstein and Mayeda, 1954). Experiments using this technique showed that equilibrium was attained in samples of normal salinity in less than 24 hr. As a result of uncertainty regarding the precise correction factors to apply for the presence of dissolved salts (Gonfiantini, 1986), I have not corrected our data for these effects. Reproducibility of oxygen isotopic analyses, determined by replicate analyses of 16 standards within a single batch of equilibrations, is $\pm 0.1\%$.

Chlorinities were measured in the waters at the time of collection by titration with AgNO_3 and standardized using IAPSO (International Association of Physical Sciences Organization) seawater. The reproducibility of this method is approximately 1‰.

A portion of the sediment cake was disaggregated and sieved into three size fractions. The foraminifer *Globigerinoides ruber* was selected from the <120 and >63 μm size fractions. Between 5 to 10 individuals were analyzed for their stable oxygen and carbon isotopic composition using an automated dissolution method at 90°C (Swart et al., 1991). The external reproducibility of this method determined by replicate analysis of standards is $\pm 0.02\%$ for both C and O.

The isotopic ratios of CO_2 for both the equilibrations and dissolutions were determined using a Finnigan-MAT 251 in the Stable Isotope Laboratory (SIL) at the Rosenstiel School of Marine and Atmospheric Sciences, University of Miami. All data have been corrected for the usual interferences and are quoted relative to PDB for carbonate and SMOW for waters.

RESULTS

Chloride

The chloride concentration of the pore water varied between 540 and 560 mM (Fig. 2). Although a gradual increase in Cl^- can be seen down the core, the variations generally were within the analytical error of $\pm 1\%$ (Table 1) of the measurement method employed.

Alkalinity

The alkalinity data presented in the initial reports showed an initial rapid rise in alkalinity with depth from seawater values of 2.2 to approximately 3.3 mM. This value remained fairly constant to a depth of a 8 mbsf, below which it increased rapidly to a value of 7 mM at the bottom of the core (Fig. 3).

¹ McKenzie, J.A., Davies, P.J., Palmer-Julson, A., et al., 1993. *Proc. ODP, Sci. Results*, 133: College Station, TX (Ocean Drilling Program).

² Stable Isotope Laboratory, MGG/RSMAS, University of Miami, Miami, FL 33149, U.S.A.

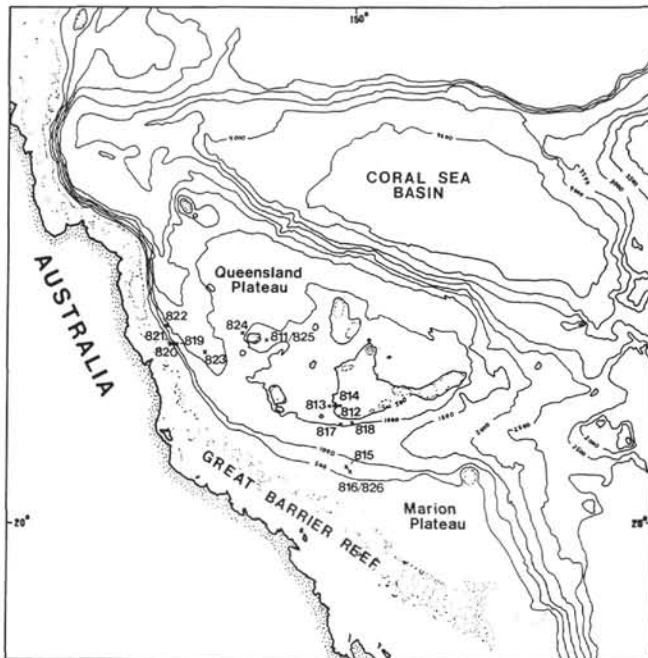


Figure 1. Location map of Site 817.

Oxygen Isotopic Composition of Pore Water

The oxygen isotopic composition of the pore water varied between approximately -0.6 and $+0.7\text{‰}$ SMOW (Fig. 4). These variations were greater than the analytical error in our measurement technique ($\pm 0.1\text{‰}$; see above) and showed systematic changes down the core. The average oxygen isotopic composition of the pore waters increases toward the base of the core.

Carbon and Oxygen Isotopic Composition of Foraminifers

The $\delta^{18}\text{O}$ of *G. ruber* varied between -2.0 and $+0.6\text{‰}$ (PDB) and showed variation, which might be interpreted as glacial-interglacial stages. The $\delta^{13}\text{C}$ was variable and was not correlated with the $\delta^{18}\text{O}$ (Fig. 5).

Revised Age Assignments

Based on the oxygen isotope stratigraphy shown in Figure 5, ages have been assigned to the various isotopic stages (Fig. 6). In this curve, I have identified most of the stages established by Imbrie et al. (1984). This chronology also agrees well with the FAD of *Emiliana huxleyi* at 25.07 mbsf (Gartner, this volume). The sedimentation rate profile calculated from these ages is shown in Figure 7.

Correlation Between *G. ruber* and Oxygen Isotopic Composition of Pore Fluids

The oxygen isotopic composition of the pore waters shows systematic variations, which below 8 mbsf, are correlatable with variations in the oxygen isotopic composition of *G. ruber*. Although this correlation is statistically significant, the significance increases substantially if the data are plotted as five sample moving averages (Fig. 8). In the lower portion of the core, the range in the $\delta^{18}\text{O}$ of the pore water varies between approximately 0.0 to 0.5‰ compared to an almost 1.5‰ variation in the isotopic composition of the foraminifers. In the upper 8 mbsf, there appears to be no correlation between the $\delta^{18}\text{O}$ of the pore fluids and foraminifers, and the magnitude of the

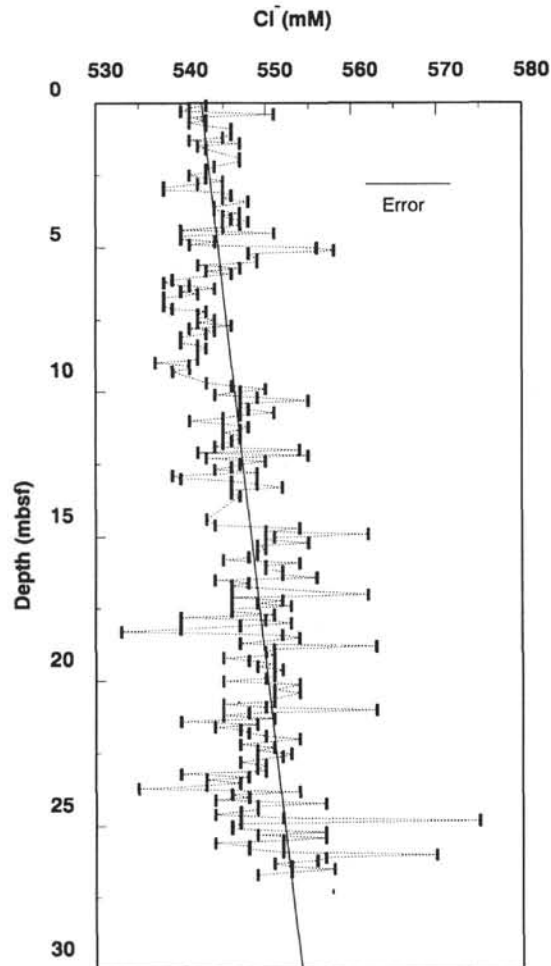


Figure 2. Chloride concentration of pore waters from Hole 817C; error bar indicates $\times 1\text{‰}$. Regression line represents trend in Cl^- concentration with depth.

variations in the oxygen isotopic composition of the pore fluids is greater (-0.5 – 0.5‰). Overall, a tendency for the pore waters to increase is seen in $\delta^{18}\text{O}$ values below 13 mbsf. This trend is similar to one seen in the Cl^- data.

DISCUSSION

The changes in the O isotopic composition of the pore fluids result from either a diagenetic signal (i.e., recrystallization of the carbonate sediment) or variations in the bottomwater signature at the time of deposition that have been subsequently modified by diffusion. A definitive method to test whether the oxygen isotopic compositions of the pore fluids are driven by carbonate recrystallization will be to measure the hydrogen isotopic composition of the pore waters, as this value is unaffected by diagenesis (Lawrence, 1989). If the δD of the pore water co-varies with that of the $\delta^{18}\text{O}$, then the signal represents a modified original bottomwater signature. If no co-variation exists between the isotopic composition of these two elements, then in all probability the variations in the $\delta^{18}\text{O}$ result from carbonate recrystallization. Certain aspects of the present data can support either of these two hypotheses. The original pore-water idea is supported by the weak correlation between Cl^- and $\delta^{18}\text{O}$ down the core. The absence of a stronger correlation is a result of scatter in the Cl^- data caused by the relatively high analytical errors involved in the technique relative to the measured change.

Support for carbonate recrystallization is evident in data collected for the Sr^{2+} concentration from Hole 817A and the alkalinity from

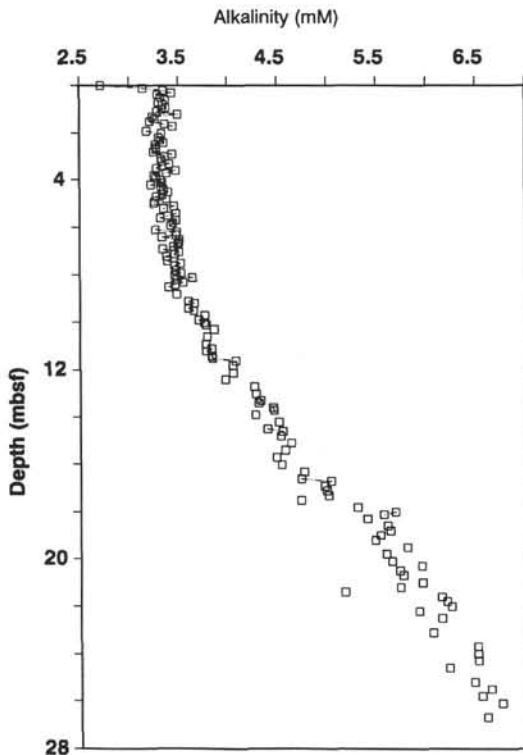
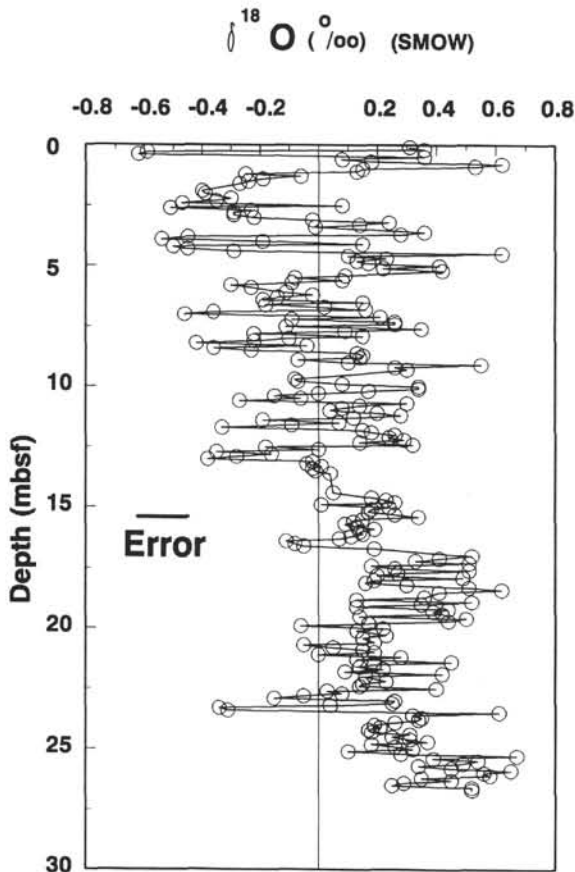
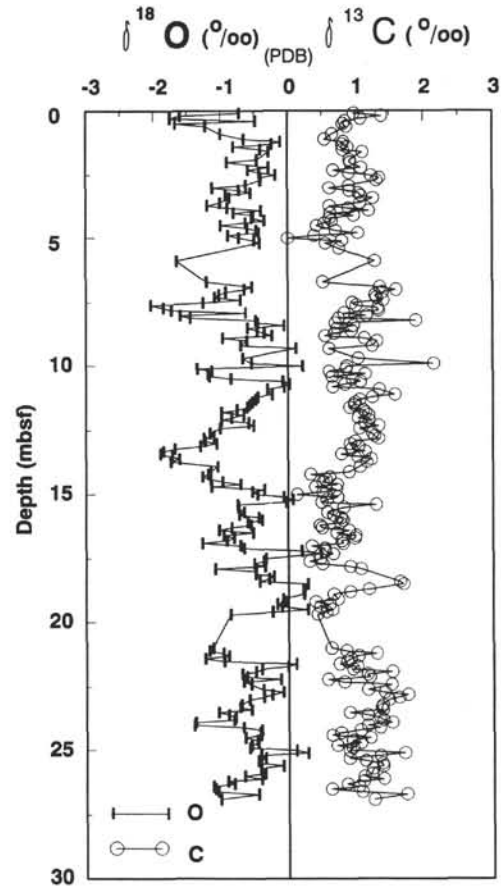


Figure 3. Alkalinity of pore waters from Hole 817C.


 Figure 4. Oxygen isotopic composition of pore waters from Hole 817C. Error bar represents $\times 0.1\%$.

 Figure 5. Carbon and oxygen isotopic compositions of *Globigerinoides ruber* from Hole 817C.

Hole 817C (Davies, McKenzie, Palmer-Julson, et al., 1990), which show evidence of extensive recrystallization throughout. The fact that the alkalinity gradient is much stronger below 8 mbsf at Hole 817C suggests that much more extensive carbonate recrystallization has occurred in this portion of the hole. This is coincidentally the region of the hole in which the $\delta^{18}\text{O}$ of the pore fluids and the $\delta^{18}\text{O}$ of the foraminifers co-vary.

The absence of co-variation in the upper portion of the hole also poses an interesting problem. Either this discrepancy is also a consequence of diagenetic alteration, or it reflects waters of differing isotopic composition at the surface and at the bottom at this time period. The latter idea can be tested by examining the isotopic composition of a benthic species (such as *Cibicides wuellerstorfi*) over this time interval. A difference in isotopic composition between the bottom and surface waters also might imply that the stratigraphy established for the upper portion of the hole may not be correct because the surface waters are being influenced by fluids of unusual isotopic composition.

The notion of rapid depletion in the pore water $\delta^{18}\text{O}$ in the upper portion of the hole being a result of diagenesis is supported by models of carbonate recrystallization such as presented by Killingley (1983). In this model, the isotopic composition of the pore water after a specified amount of recrystallization can be calculated from the following equation:

$$\delta w_{\alpha} = \frac{M_c R (\delta C_i + 10^3 (1 - \alpha_T) + M_w \delta w_i)}{M_w + M_c \alpha_T R}$$

In this equation, δw_{α} = $\delta^{18}\text{O}$ of interstitial water after recrystallization, δC_i = $\delta^{18}\text{O}$ of calcium carbonate of initial sediment, δw_{α} =

Table 1. Geochemical data from Hole 817C including stable O and C isotope data from *G. ruber*, porewater $\delta^{18}\text{O}$ and Cl measurements.

Core, section, interval (cm)	Depth (mbsf)	Age (\times k.y.)	$\delta^{13}\text{C}$ ‰	$\delta^{18}\text{O}$ ‰	$\delta^{18}\text{O}$ ‰ (SMOW)	Cl ⁻ (mM)	Core, section, interval (cm)	Depth (mbsf)	Age (\times k.y.)	$\delta^{13}\text{C}$ ‰	$\delta^{18}\text{O}$ ‰	$\delta^{18}\text{O}$ ‰ (SMOW)	Cl ⁻ (mM)	
IH-1, 0	0.1	0	0.98	-0.72	0.3	543	2H-1, 30	8.5	142.9	0.73	-0.60	-0.2	543	
IH-1, 10	0.2	1.2	1.39	-1.60	0.4	541	2H-1, 40	8.6	146.6	0.94	-0.46	0.1	542	
IH-1, 20	0.3	2.4	1.08	-1.75	-0.6	540	2H-1, 50	8.7	150.3	0.69	-0.35	0.1	542	
IH-1, 30	0.4	3.5	0.85	-0.48	-0.6	551	2H-1, 60	8.8	154.1	0.55	-0.24	0.1	542	
IH-1, 40	0.5	4.7	0.82	-1.67	0.4	541	2H-1, 70	8.9	157.8	1.13	-0.97	-0.1	542	
IH-1, 50	0.6	5.9	0.87	-1.22	0.1	543	2H-1, 80	9.0	161.5	1.32	-0.61	0.1	537	
IH-1, 60	0.7	7.1			0.2	541	2H-1, 90	9.1	165.2			0.5	541	
IH-1, 70	0.8	8.3			0.6	543	2H-1, 100	9.2	168.9	1.25	-0.70	0.3	541	
IH-1, 80	0.9	9.5	0.66	-1.00	0.5	546	2H-1, 110	9.3	172.7	0.61	0.12	0.3	539	
IH-1, 90	1.0	10.6			0.1	546	2H-2, 0	9.7	176.4	1.04	-0.67	-0.1	543	
IH-1, 100	1.1	11.8	0.55	-0.65	0.1	546	2H-2, 10	9.8	180.1			-0.1	546	
IH-1, 110	1.2	13.0	0.83	-0.11	-0.3	545	2H-2, 20	9.9	183.8	2.15	-0.54	0.1	550	
IH-1, 120	1.3	16.4	0.81	-0.24	-0.1	541	2H-2, 30	10.0	187.6	0.87	0.22	0.3	547	
IH-1, 130	1.4	19.9	0.89	-0.81	-0.2	547	2H-2, 40	10.1	195.0	0.86	-1.35	0.3	544	
IH-1, 140	1.5	23.3	0.82	-0.41	-0.2	542	2H-2, 50	10.2	196.3	0.61	-1.13	0.2	549	
IH-2, 0	1.6	26.8	1.11	-0.28	-0.3	543	2H-2, 60	10.3	197.5	1.14	-1.19	0.0	555	
IH-2, 10	1.7	30.2			-0.1	547	2H-2, 70	10.4	198.8	0.65	-1.17	-0.2	547	
IH-2, 20	1.8	33.7					2H-2, 80	10.5	200.1	0.95	-0.85	-0.1	547	
IH-2, 30	1.9	37.1	0.92	-0.46	-0.4	547	2H-2, 90	10.6	201.4	1.07	-0.08	-0.3	548	
IH-2, 40	2.0	40.6	0.93	-0.90	-0.4	547	2H-2, 100	10.7	202.6	0.84	0.02	0.3	551	
IH-2, 50	2.1	44.0					2H-2, 110	10.8	203.9	0.66	-0.06	0.1	547	
IH-2, 60	2.2	47.4	1.09	-0.28	-0.3	544	2H-2, 120	10.9	205.2	1.35	-0.31	0.1	545	
IH-2, 70	2.3	50.9	0.68	-0.59	-0.4	543	2H-2, 130	11.0	206.5			0.0	541	
IH-2, 80	2.4	54.3	0.91	-0.42	-0.5	543	2H-2, 140	11.1	207.7	1.58	-0.24	0.2	545	
IH-2, 90	2.5	57.8	1.24	-0.18	0.1	541	2H-3, 0	11.2	209.0	1.25	-0.45	0.3	548	
IH-2, 100	2.6	61.2	1.36	-0.40	-0.5	543	2H-3, 10	11.3	210.3	1.06	-0.48	0.1	547	
IH-2, 110	2.7	64.7	1.32	-0.41	-0.2	545	2H-3, 20	11.4	211.5	0.99	-0.53	-0.2	545	
IH-2, 120	2.8	68.1			-0.3	542	2H-3, 30	11.5	212.8	0.98	-0.57	0.1	547	
IH-2, 130	2.9	71.6	0.91	-0.62	-0.3	538	2H-3, 40	11.6	214.1	0.91	-0.61	-0.1	547	
IH-2, 140	3.0	75.0	0.62	-1.12	-0.2	538	2H-3, 50	11.7	215.4	1.11	-0.76	-0.3	546	
IH-3, 0	3.1	76.0	0.91	-0.73	0.0	545	2H-3, 60	11.8	216.6	1.15	-0.99	0.1	545	
IH-3, 10	3.2	77.1	1.05	-0.56	0.2	546	2H-3, 70	11.9	217.9	1.19	-0.66	0.2	544	
IH-3, 20	3.3	78.1	1.08	-0.93	0.1	545	2H-3, 80	12.0	219.2	1.04	-0.84	0.3	554	
IH-3, 30	3.4	79.2	1.26	-0.87	0.0	548	2H-3, 90	12.1	220.5	1.20	-0.99	0.2	542	
IH-3, 40	3.5	80.2			0.2	545	2H-3, 100	12.2	221.7	1.14	-0.58	0.3	555	
IH-3, 50	3.6	81.2	1.07	-1.01	0.4	544	2H-3, 110	12.3	223.0	1.34	-0.51	0.1	543	
IH-3, 60	3.7	82.3	0.62	-1.20	0.3	544	2H-3, 120	12.4	224.3	1.06	-1.01	0.3	550	
IH-3, 70	3.8	83.3	0.90	-0.90	-0.4	547	2H-3, 130	12.5	225.5			-0.2	547	
IH-3, 80	3.9	84.4	1.20	-0.40	-0.5	545	2H-3, 140	12.6	226.8	1.25	-1.16	0.0	546	
IH-3, 90	4.0	85.4	0.63	-0.81	-0.2	546	2H-4, 0	12.7	228.1	1.28	-1.10	-0.3	544	
IH-3, 100	4.1	86.4	0.98	-0.51	0.2	548	2H-4, 10	12.8	229.4	1.34	-1.25	-0.2	549	
IH-3, 110	4.2	87.5	0.62	-0.54	-0.5	547	2H-4, 20	12.9	230.6	0.99	-1.23	-0.3	539	
IH-3, 120	4.3	88.5	0.65	-0.35	-0.5	545	2H-4, 30	13.0	231.9	0.92	-1.06	-0.4	540	
IH-3, 130	4.4	89.5	0.54	-0.63	-0.3	540	2H-4, 40	13.1	233.2	1.04	-1.30	0.0	546	
IH-3, 140	4.5	90.6	0.43	-1.00	0.6	551	2H-4, 50	13.2	234.5	0.94	-1.68	0.0	549	
IH-4, 0	4.6	91.6			-0.60	0.1	540	2H-4, 60	13.3	235.7	1.14	-1.85	0.0	552
IH-4, 10	4.7	92.7	0.71	-0.47	0.2	540	2H-4, 70	13.4	237.0	0.79	-1.89	0.0	546	
IH-4, 20	4.8	93.7	1.04	-0.43	0.1	544	2H-4, 80	13.5	238.3	1.03	-1.72	0.0	546	
IH-4, 30	4.9	94.7	0.39	-0.89	0.2	541	2H-4, 90	13.6	239.5	1.23	-1.61	0.0	547	
IH-4, 40	5.0	95.8	0.00	-0.73	0.4	556	2H-4, 100	13.7	240.8	1.16	-1.74			
IH-4, 50	5.1	96.8	0.80	-0.50	0.2	558	2H-4, 110	13.8	242.1					
IH-4, 60	5.2	97.9	0.56	-0.42	0.4	548	2H-4, 120	13.9	243.4	1.06	-1.05			
IH-4, 70	5.3	98.9			0.5	553	2H-4, 140	14.1	244.6	0.90	-1.15			
IH-4, 80	5.4	99.9			0.1	549	2H-5, 0	14.2	245.9	0.33	-1.19			
IH-4, 90	5.5	101.0			-0.1	549	2H-5, 10	14.3	247.2	0.61	-1.27			
IH-4, 100	5.6	102.0			0.1	542	2H-5, 20	14.4	248.5	0.55	-1.15	0.0	543	
IH-4, 110	5.7	103.1			-0.1	547	2H-5, 30	14.5	251.0	0.51	-0.98			
IH-4, 120	5.8	104.1			-0.3	543	2H-5, 40	14.6	251.5	0.72	-0.71	0.2	544	
IH-4, 130	5.9	105.1	1.29	-1.65	-0.2	546	2H-5, 50	14.7	252.0	0.40	-1.14	0.2	554	
IH-4, 140	6.0	106.2					2H-5, 60	14.8	252.5	0.71	-0.36	0.3	550	
IH-5, 0	6.1	107.2			-0.1	539	2H-5, 70	14.9	253.0	0.51	-0.53	0.0	562	
IH-5, 10	6.2	108.3			0.0	538	2H-5, 80	15.0	253.5	0.13	-0.46	0.2	551	
IH-5, 20	6.3	109.3			-0.1	541	2H-5, 90	15.1	254.0	0.73	-0.07	0.2	550	
IH-5, 30	6.4	110.3			-0.2	544	2H-5, 100	15.2	254.5	0.57	0.07	0.2	555	
IH-5, 40	6.5	111.4			0.1	540	2H-5, 110	15.3	255.0	0.49	-0.03	0.3	549	
IH-5, 50	6.6	112.4			-0.2	542	2H-5, 120	15.4	255.5	1.30	-0.75	0.3	550	
IH-5, 60	6.7	113.5	0.52	-1.21	0.0	538	2H-5, 130	15.5	255.9	0.82	-0.74	0.1	549	
IH-5, 70	6.8	114.5			0.2	538	2H-5, 140	15.6	256.4			0.1	549	
IH-5, 80	6.9	115.5	1.36	-0.54	-0.4	538	2H-6, 0	15.7	256.9	0.58	-0.66	0.1	548	
IH-5, 90	7.0	116.6	1.60	-0.65	-0.5	538	2H-6, 10	15.8	257.4	0.67	-0.73	0.1	545	
IH-5, 100	7.1	117.6	1.40	-0.93	0.2	539	2H-6, 20	15.9	257.9	0.78	-0.44	0.2	554	
IH-5, 110	7.2	118.6	1.29	-1.03	-0.1	543	2H-6, 30	16.0	258.4	0.81	-0.39	0.1	550	
IH-5, 120	7.3	119.7	1.31	-1.09	0.3	542	2H-6, 40	16.1	258.9	0.77	-0.60	0.2	550	
IH-5, 130	7.4	120.7	1.41	-0.71	0.3	542	2H-6, 50	16.2	259.4	0.47	-0.55	0.1	552	
IH-5, 140	7.5	121.8	0.95	-1.26	-0.1	544	2H-6, 60	16.3	259.9	0.50	-0.84	0.1	552	
IH-6, 0	7.6	122.8	1.01	-2.04	0.3	542	2H-6, 70	16.4	260.4	0.90	-1.03	-0.1	556	
IH-6, 10	7.7	123.8	1.33	-1.85	0.1	546	2H-6, 80	16.5	260.9	0.72	-0.52	-0.1	544	
IH-6, 20	7.8	124.9	1.34	-1.73	-0.2	541	2H-6, 90	16.6	261.4	1.00	-0.96	-0.1	548	
IH-6, 30	7.9	125.9	0.83	-0.63	0.2	544	2H-6, 100	16.7	261.9	0.99	-0.80	0.2	546	
IH-6, 40	8.0	127.0	1.16	-1.60	-0.1	543	2H-6, 110	16.8	262.4	0.79	-0.91			
IH-6, 0	8.1	128.0	0.75	-1.45	-0.2	540	2H-6, 120	16.9	262.9	0.81	-1.27			
2H-1, 0	8.2	131.7	1.89	-0.48	-0.4	540	2H-6, 130	17.0	263.4	0.35	-0.71	0.5	562	
2H-1, 10	8.3	135.4	0.70	-0.45	0.0	540	2H-6, 140	17.1	263.9	0.54	-0.66	0.4	546	
2H-1, 20	8.4	139.2	0.97	-0.06	-0.4	542	2H-7, 0	17.2	264.4	0.54	0.20	0.3	552	

Table 1 (continued).

Core, section, interval (cm)	Depth (mbsf)	Age (× k.y.)	$\delta^{13}\text{C}$ ‰	$\delta^{18}\text{O}$ ‰	$\delta^{18}\text{O}$ ‰ (SMOW)	Cl ⁻ (mM)	Core, section, interval (cm)	Depth (mbsf)	Age (× k.y.)	$\delta^{13}\text{C}$ ‰	$\delta^{18}\text{O}$ ‰	$\delta^{18}\text{O}$ ‰ (SMOW)	Cl ⁻ (mM)
2H-7, 10	17.3	264.8	0.66	0.48	0.5	549	3H-3, 120	22.2	289.1	0.58	-0.12	0.2	547
2H-7, 20	17.4	265.3			0.2	553	3H-3, 130	22.3	289.6	0.82	-0.67	0.1	551
2H-7, 30	17.5	265.8	0.47	-0.34	0.3	546	3H-3, 140	22.4	290.1	1.52	-0.56	0.1	549
2H-7, 40	17.6	266.3	0.31	-0.37	0.5	546	3H-3, 0	22.5	290.6			0.4	553
2H-7, 50	17.7	266.8	0.50	-0.51	0.3	551	3H-4, 10	22.6	291.1	1.17	-0.38	0.0	552
2H-7, 60	17.8	267.3	0.91	-0.35	0.2	540	3H-4, 20	22.7	291.6	1.42	-0.08	0.1	549
2H-7, 70	17.9	267.8	1.07	-1.09	0.5	550	3H-4, 30	22.8	292.1	1.76	-0.25	0.0	547
3H-1, 0	18.0	268.3		-0.48	0.2	553	3H-4, 40	22.9	292.5	1.63	-0.37	-0.2	550
3H-1, 10	18.1	268.8		-0.49	0.2	547	3H-4, 50	23.0	293.0	1.48	-0.58	0.3	549
3H-1, 20	18.2	269.3		-0.22	0.3	540	3H-4, 60	23.1	293.5			0.2	550
3H-1, 30	18.3	269.8		-0.29	0.5	533	3H-4, 70	23.2	294.0	1.39	-0.70	0.0	540
3H-1, 40	18.4	270.3	1.65	-0.43	0.6	552	3H-4, 80	23.3	294.5	1.37	-0.72	-0.3	548
3H-1, 0	18.5	270.8	1.70	0.29	0.4	554	3H-4, 90	23.4	295.0	1.39	-0.55	-0.3	543
3H-1, 60	18.6	271.3			0.3	550	3H-4, 100	23.5	295.5	0.90	-1.04	0.6	547
3H-1, 70	18.7	271.8	1.19	0.22	0.4	547	3H-4, 110	23.6	296.0	1.16	-0.89	0.3	543
3H-1, 80	18.8	272.3	0.91	0.24	0.1	563	3H-4, 120	23.7	296.5	1.35	-0.79	0.3	535
3H-1, 90	18.9	272.8	0.67	0.23	0.5	551	3H-4, 130	23.8	297.0	1.40	-0.81	0.3	554
3H-1, 100	19.0	273.3			0.4	550	3H-4, 140	23.9	297.5	1.53	-1.38	0.3	546
3H-1, 110	19.1	273.8	0.73	-0.08	0.1	551	3H-5, 0	24.0	298.0	1.17	-1.40	0.2	548
3H-1, 120	19.2	274.2	0.40	-0.05	0.4	545	3H-5, 10	24.1	298.5	1.35	-0.67	0.2	544
3H-1, 130	19.3	274.7	0.61	-0.17	0.4	548	3H-5, 20	24.2	299.0	1.06	-0.40	0.2	557
3H-1, 140	19.4	275.2	0.47	-0.10	0.4	551	3H-5, 30	24.3	299.5	0.77	-0.43	0.2	549
3H-2, 0	19.5	275.7	0.65	0.29	0.1	549	3H-5, 40	24.4	300.0	0.64	-0.42	0.3	549
3H-2, 10	19.6	276.2	0.56	-0.24	0.5	552	3H-5, 50	24.5	300.5	1.20	-0.65	0.3	547
3H-2, 20	19.7	276.7	0.43	-0.86	0.4	551	3H-5, 60	24.6	301.0	0.94	-0.47	0.3	544
3H-2, 30	19.8	277.2			0.2	551	3H-5, 70	24.7	301.5	1.06	-0.46	0.4	552
3H-2, 40	19.9	277.7			-0.1	550	3H-5, 80	24.8	301.9	0.71	-0.56	0.2	575
3H-2, 50	20.0	278.2			0.2	545	3H-5, 90	24.9	302.4	0.94	-0.58	0.3	547
3H-2, 60	20.1	278.7			0.1	554	3H-5, 100	25.0	302.9	0.89	0.11	0.3	546
3H-2, 70	20.2	279.2					3H-5, 110	25.1	303.4	1.71	0.28	0.1	546
3H-2, 80	20.3	279.7			0.2	551	3H-5, 120	25.2	303.9	1.35	-0.42	0.3	557
3H-2, 90	20.4	280.2			0.2	554	3H-5, 130	25.3	304.4	0.89	-0.35	0.7	549
3H-2, 100	20.5	280.7					3H-5, 140	25.4	304.9	1.13	-0.46	0.4	557
3H-2, 110	20.6	281.2			0.2	551	3H-6, 0	25.5	305.4	1.38	-0.43	0.5	552
3H-2, 120	20.7	281.7			-0.1	551	3H-6, 10	25.6	305.9	1.39	-0.09	0.5	544
3H-2, 130	20.8	282.2			0.0	545	3H-6, 20	25.7	306.4	1.24	-0.42	0.3	548
3H-2, 140	20.9	282.7			0.1	550	3H-6, 30	25.8	306.9			0.5	548
3H-3, 0	21.0	283.2	0.63	-1.12	0.2	563	3H-6, 40	25.9	307.4	1.22	-0.36	0.7	552
3H-3, 10	21.1	283.6	0.85	-1.18	0.0	548	3H-6, 50	26.0	307.9	1.11	-0.66	0.6	570
3H-3, 20	21.2	284.1	1.30	-0.97	0.3	545	3H-6, 60	26.1	308.4	1.40	-0.41	0.6	557
3H-3, 30	21.3	284.6	1.03	-0.89	0.1	551	3H-6, 70	26.2	308.9	1.10	-0.91	0.3	556
3H-3, 40	21.4	285.1	0.91	-1.24	0.4	540	3H-6, 80	26.3	309.4	0.86	-0.81	0.4	551
3H-3, 50	21.5	285.6	0.86	-0.96	0.2	549	3H-6, 90	26.4	309.9	1.03	-1.12	0.3	553
3H-3, 60	21.6	286.1	0.75	0.11	0.1	544	3H-6, 100	26.5	310.4	0.63	-1.09	0.3	558
3H-3, 70	21.7	286.6	1.01	-0.01	0.2	547	3H-6, 110	26.6	310.8	1.08	-1.05	0.5	553
3H-3, 80	21.8	287.1	0.95	-0.40	0.1	548	3H-6, 120	26.7	311.3	1.74	-0.45	0.5	549
3H-3, 90	21.9	287.6	1.53	-0.49	0.4	550	3H-6, 130	26.8	311.8				
3H-3, 100	22.0	288.1	1.16	-0.69	0.2	554	3H-6, 140	26.9	312.3	1.26	-1.01		549
3H-3, 110	22.1	288.6	1.20	-0.62									

$\delta^{18}\text{O}$ of interstitial waters before reaction, M_c = mole fraction of oxygen in carbonate sediment, M_w = mole fraction of oxygen in pore waters, R = percentage of recrystallization, and α = fractionation factor between calcite-water.

In the case for Hole 817C, I have used a bottom temperature of 10°C, a geothermal gradient of 50°C/km (data from Davies, McKenzie, Palmer-Julson, et al., 1990), an initial sediment isotopic composition of -2‰ (PDB), a water isotopic composition of 0.5‰ (SMOW) (Fig. 9), a porosity of 50%, and a carbonate content of 80%. If in this case one assumes that the recrystallized calcium carbonate does not re-equilibrate with the pore fluids, then the isotopic composition of the pore waters will rapidly become depleted with depth. This is similar to the case at Hole 817C. As may be observed from this simplistic example the result of initial recrystallization is to produce pore waters that are isotopically depleted. If the pore waters do not continue to react with the carbonate, then the isotopic composition of the fluid should in the absence of diffusion remain at approximately -1.0‰. However, continued recrystallization of the sediment may cause the isotopic composition of the fluids to co-vary with the foraminifers, as is observed in the lower portion of Hole 817C.

The origin of these $\delta^{18}\text{O}$ values will be further tested by (1) constructing a mathematical model that will account for not only

diffusion, but also advection, and carbonate recrystallization, (2) measurement of the δD of the pore waters, and (3) measurement of the isotopic composition of benthic foraminifers from the cores.

CONCLUSIONS

There is a co-variance between the oxygen isotopic composition of *G. ruber* and the pore waters below 8 mbsf. The magnitude of the variation in the $\delta^{18}\text{O}$ of the waters is approximately 30‰ of that seen in the $\delta^{18}\text{O}$ of the foraminifers, suggesting that diffusion and perhaps recrystallization have altered the isotopic compositions. Circumstantial evidence exists to support both of these hypotheses, and the eventual cause will only be revealed by (1) analyzing the hydrogen isotopic composition of the pore fluids, (2) mathematically modeling the processes of carbonate recrystallization, diffusion, and advection, and (3) investigating the isotopic composition of the benthic foraminifers.

ACKNOWLEDGMENTS

The author would like to thank the technicians, scientists, and crew of Leg 133 for continued help throughout the cruise. Joe Powers, Joe DeMorett, and Scott Chaffey are especially thanked for their help in

the chemistry laboratory. Alex Isern, Danny Muller, and Judy McKenzie provided friendship and discussion throughout. I would especially like to thank all those who helped with the marathon squeezing effort. In addition to those mentioned above, Christian Betzler, George Dix, David Feary, Craig Glenn, Jose Martin, Lucien Montaggioni, and Chris Pigram manned the presses during the 36-hr squeezing effort. Help with the shore-based analyses was provided by Amel Saied, Jeff Abell, and Jim Leder. Thanks to Michael Lopez and Yvette Alger for many hours of selecting foraminifers. Conversations with Geoff Haddad, Andre Droxler, Larry Peterson, and Pam Reid helped with the interpretation of the oxygen isotope stratigraphy.

REFERENCES*

Davies, P.J., McKenzie, J.A., Palmer-Julson, A., et al., 1991. *Proc. ODP, Init. Repts.*, 133: College Station, TX (Ocean Drilling Program).
 Epstein, S., and Mayeda, T., 1953. Variation of ^{18}O content of waters from natural sources. *Geochim. Cosmochim. Acta*, 42:213-224.
 Gonfiantini, R., 1986. Environmental isotopes in lake studies. In Fritz, P., and Fontes, J.Ch. (Eds.) *Handbook of Environmental Isotope Geochemistry, Vol 2.*, (Elsevier), 113-168.
 Imbrie, J., Hays, J.D., Martinson, D.G., McIntyre, A., Mix, A., Morley, J.J., Pisias, N.G., Prell, W.L., and Shackleton, N.J., 1984. The orbital theory of

Pleistocene climate: support from a revised chronology of the marine $\delta^{18}\text{O}$ record. In Berger, A.L., et al. (Eds.), *Milankovitch and Climate, Pt. 1*: New York (Reidel Publ. Co.), 269-305.
 Killingley, J.S., 1983. Effects of diagenetic recrystallization on $^{18}\text{O}/^{16}\text{O}$ values of deep-sea sediments. *Nature*, 301:594-597.
 Lawrence, J.R., 1989. The stable isotope geochemistry of deep-sea pore water. In Fritz, P., and Fontes, J.Ch. (Eds.), *Handbook of Environmental Isotope Geochemistry, Vol. 3*: New York (Elsevier), 317-356.
 Manheim, F.T., and Sayles, F.L., 1974. Composition and origin of interstitial waters of marine sediments based on deep sea drill cores. In Goldberg, E.D., *The Sea, Vol. 5*: New York (Wiley), 527-568.
 Swart, P.K., Burns, S.J., and Leder, J.J., 1991. Fractionation of the stable isotopes of O and C in CO_2 during the reaction of calcite with phosphoric acid as a function of temperature and technique. *Chem. Geol. (Isotope Geosci. Sect.)*, 86:89-96.

* Abbreviations for names of organizations and publication titles in ODP reference lists follow the style given in *Chemical Abstracts Service Source Index* (published by American Chemical Society).

Date of initial receipt: 21 April 1992
 Date of acceptance: 10 December 1992
 Ms 133SR-260

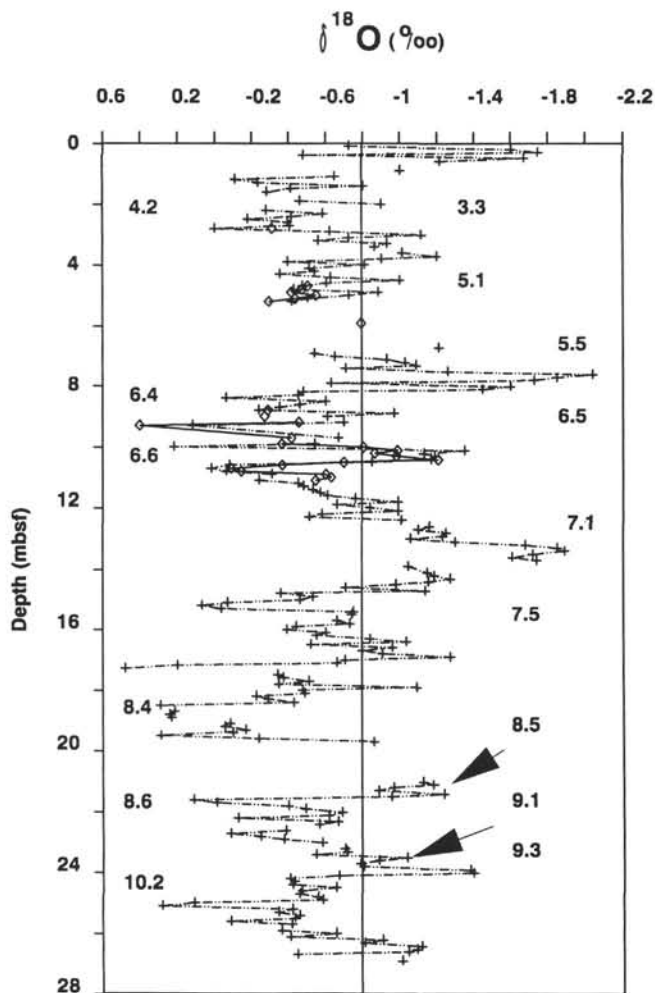


Figure 6. Oxygen isotopic stratigraphy of Hole 817C. The diamonds and the solid lines represent replicated data. Stage numbers are from Imbrie et al. (1984).

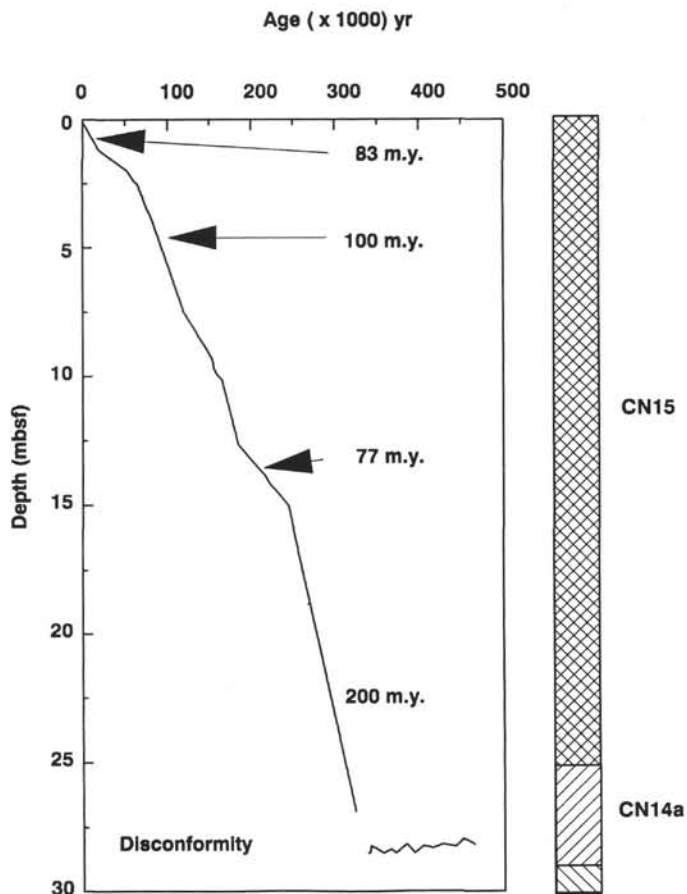


Figure 7. Sedimentation rate for Hole 817C. Nannofossil zones are from Gartner (this volume).

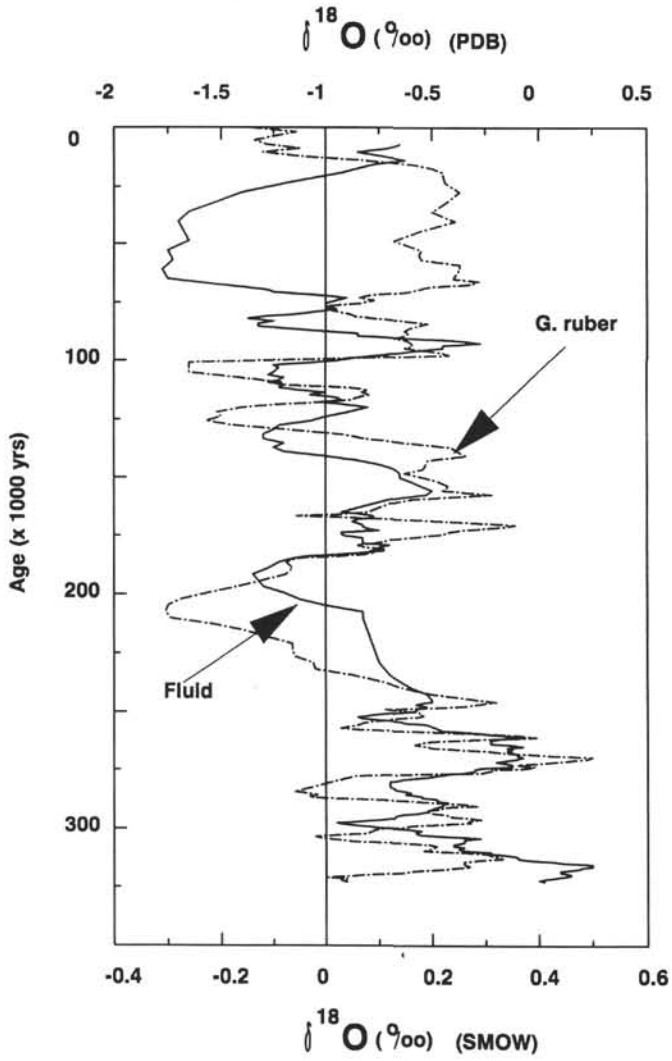


Figure 8. Smoothed oxygen isotopic composition of the pore waters compared to *G. ruber* from Hole 817C.

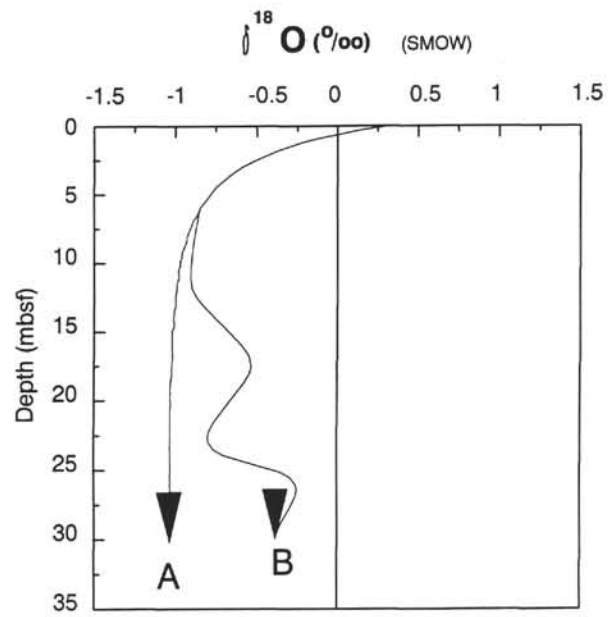


Figure 9. Theoretical effect of carbonate recrystallization on the $\delta^{18}\text{O}$ of pore waters using the following parameters ($\delta^{18}\text{O}_i = -2\text{‰}$ (PDB); $\delta^{18}\text{O}_w = +0.5\text{‰}$ (SMOW); $dt/dz = 50^\circ\text{C}/\text{km}$; and bottom temperature = 10°C). Line (A) represents pore water which initially experiences a great deal of recrystallization and little subsequent isotopic exchange with the sediments. Line (B) shows pore water which continues to isotopically exchange with the sediments.